Study on Metamorphic Rolling Mechanism for Metal Hybrid Additive Manufacturing

Haiou Zhang*[a], Daoman Rui[a], Yang Xie[a], Guilan Wang[b]

[a]State Key Laboratory of Digital Manufacturing Equipment and Technology, Huazhong University of Science and Technology, Wuhan 430074, PR China

[b]State Key Laboratory of Materials Processing and Die & Mould Technology, Huazhong University of Science and Technology, Wuhan 430074, PR China

Accepted August 16th 2013

Abstract

The uneven of the surface shaped by overlapping beads has been observed during metal additive manufacturing (AM). These uneven surfaces have a cumulative effect on the accuracy of the component in the Z-direction. Conventionally, each layer was face milled to solve the problem, which resulted in material and time wastes. In this paper, the metamorphic mechanism was introduced to metal additive manufacturing and a novel metamorphic rolling mechanism with three rollers was developed. It configuration can change according to the feature of the part to rolling the deposition upper or lateral surfaces. The influence of rolling force and rolling temperature on the shape of bead was studied. Optimal rolling parameters were obtained to control the height and width of overlapping beads. In addition, it is worthwhile to mention that the hybrid deposition and rolling method will be beneficial to refine grain, avoid the hot crack and improve the mechanical properties of parts.

Introduction

Additive manufacturing using arc welding as the energy source has drawn a significant research interest owing to its low cost, high efficiency and simple equipment [1, 2]. Generally, the arc welding based additive manufacturing process is composed of several procedures including establishing the part 3D model, deposition path planning for each layer, and stacking up of beads layer by layer.

The uneven of the surfaces formed by overlapping beads has been observed by many authors. These uneven surfaces will have a cumulative effect on the accuracy of the component in the Z-direction. At present, many researches for controlling the geometries of the deposited beads during arc welding deposition were carried out. Jun et al. developed a computer vision-sensing system for closed loop control of bead width[3].Yu et al. and Kim et al. studied the effects of process parameters on bead width and height using fuzzy regression method and neural networks, respectively [4,5]. Cao et al. and Suryakumar et al. constructed the model of the single bead profile which was used to determine the overlapping distance of adjacent beads in the gas metal arc welding (GMAW) based additive manufacturing process[6,7]. These methods were beneficial

*Corresponding author E-mail : zholab@mail.hust.edu.cn (Haiou Zhang),wgllab@mail.hust.edu.cn.

to increase the process stability. However, they could not obtain flat surface due to the effect of melted metal surface tension. On the other hand, hybrid deposition and milling approach was developed to improve the surface accuracy and quality during AM process [8-10]. Each layer was face milled to remove scallops and stack up of errors, which resulted in material and time wastes of the process.

In this paper，a novel hybrid additive manufacturing approach integrating arc welding and continuous rolling was studied to control the shape of the bead and the overlapping beads. A metamorphic rolling mechanism (MRM) with three rollers was designed to control the width or height of the beads and its configuration can change according to the feature of the part.

Hybrid deposition and rolling mechanism design

The concept of metamorphic mechanisms was proposed in 1998 by Dai in the study of packing cartons and their equivalent mechanisms [11]. The metamorphic mechanism has the characteristics of multi-configuration, variable constraints, and multi-function. It has the ability to change configuration sequentially from one to another as a resultant change of the number of effective links and topological structure to achieve different tasks following its working conditions and requirements [12].

The metamorphic mechanism was introduced to design the hybrid deposition and rolling mechanism for its multi-configuration characteristic. As shown in Fig.1, the designed metamorphic rolling mechanism is comprised of one horizontal roller and two vertical rollers. The horizontal roller is adopted to deform the beads in the height direction and to flatten the upper surface of the beads. The vertical roller is used to deform the beads in the width direction giving rise to the formation of a flat lateral surface. The rolling mechanism can change its configuration according to the part features including:

(i) One roller work condition is for multi-beaded part. As shown in Fig.1a, the horizontal roller is used to roll the upper surface of the bead while both of the vertical rollers are raising.

(ii) Two rollers work condition is for outer edges of multi-beaded part. As shown in Fig.1b, the horizontal roller is used to roll the upper surface of the bead. One vertical roller is lowered to roll the lateral surface of the bead while the other vertical roller is raising.

(iii) Three rollers work condition is for thin-walled part. The horizontal roller is used to roll the upper surface of the bead while both of the vertical rollers were lowered to roll the lateral surfaces of the bead, and moreover, the vertical rollers can translate at the horizontal direction according to the thickness of the walls, as seen in Fig. 1c and Fig. 1d.

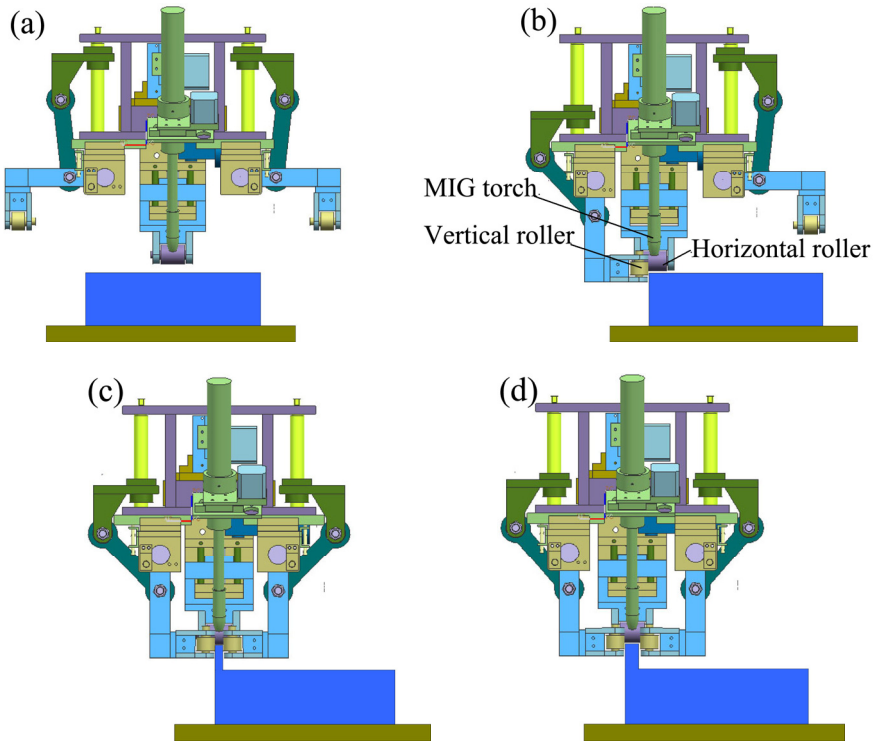

Fig.1 Simulation of metamorphic rolling mechanism for different work condition, (a) one roller, (b) two rollers, (c) three rollers for thin wall with thickness of 6 mm, (d) three rollers for thin wall with thickness of 10 mm

As shown in Fig.2, to satisfy the above rolling demands during the additive manufacturing process, metamorphic mechanisms was applied to the innovative design of the vertical rollers which can change its configuration. Three working-phase mechanisms were constructed for the multiple tasks of the vertical rollers such as raising, lowing and translating. The advantage of the metamorphic vertical roller mechanism is that one driving motor can finish these motion functions. As shown in Fig.2a, motion I is the active motion which can be realized by screw-nut pairs driving by a stepping motor.

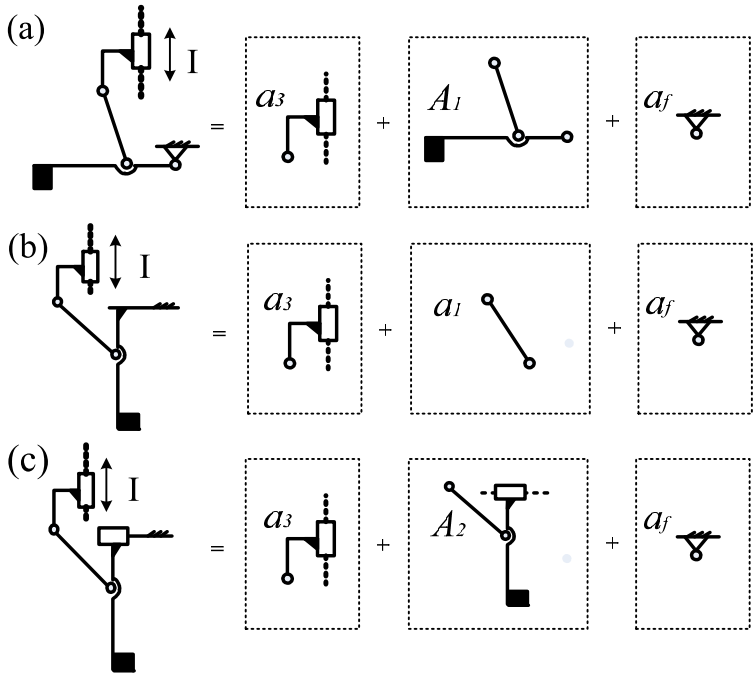

Fig.2 Configurations of working-phase vertical roll mechanism, (a) raising, (b) lowing, (c) translating

To conceive an appropriate source-metamorphic mechanism of vertical roller which contained the three working-phase mechanisms, the biological modeling and genetic evolution method given by Zhang, et al. was used [13]. The working-phase mechanisms and source-metamorphic mechanism can be modeled as follows:

$$^{i}M = [a_i; A_i; a_f] \tag{1}$$

$$^{S}M = [a_i; A_i; a_f] \tag{2}$$

Where ^{i}M and ^{S}M represents working-phase mechanisms and source-metamorphic mechanism, respectively, a_i stands for the active gene, A_i is the expression of metamorphic cell, and a_f represents the frame gene.

Thus, the biological modeling for the working-phase mechanisms of vertical roller in Fig. 2 can be expressed as follows:

$$^{1}M = [a_3; A_1; a_f] \tag{3}$$

$$^{2}M = [a_3; a_1; a_f] \tag{4}$$

$$^{3}M = [a_3; A_2; a_f] \tag{5}$$

Then, the generation of ^{S}M from the genetic evolution synthesis can be expressed as Eq. (6).

$$^{S}M = (^{1}M \cup ^{2}M) \cup ^{3}M \tag{6}$$

$$= [a_3; A_1 \cup a_1; a_f \cup a_f] \cup {}^3M$$

$$= [a_3; A_1; a_f] \cup [a_3; A_2; a_f]$$

$$= [a_3; A_1 \cup A_2; a_f \cup a_f]$$

$$= [a_3; a_1; A_2; a_f]$$

From the biological modeling of Eq. (6), the source-metamorphic mechanism diagram of vertical roller was established, as shown in Fig.3. The three-dimensional structure modeling of the metamorphic vertical roller was designed using software UG according to the source-metamorphic mechanism diagram, which can complete the transition between these working-phase mechanisms by designed metamorphic ways.

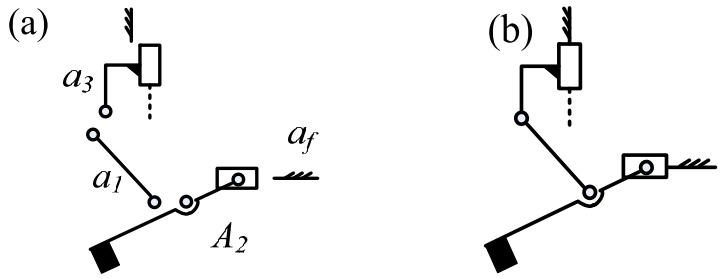

Fig.3 The source-metamorphic mechanism diagram of vertical roller, (a) genetic components of vertical roller, (b) diagram of vertical roller

Experimental conditions

The metal inert gas (MIG) welding based deposition and rolling additive manufacturing system is shown in Fig.4, which includes a computer numerical control (CNC) machine, a DIGI@WAVE-500 welding power supply, a welding torch, the designed metamorphic rolling mechanism, and a PLC for the rolling mechanism motion control and data acquisition (rolling temperature and rolling force). The metamorphic rolling mechanism is located behind the MIG welding gun and they move synchronously at the welding speed. The distance L between the welding electrode and the roll along the deposition direction can be adjusted by movement 1 to obtain proper rolling temperature. The numerical control (NC) programs generated by software are used to control the CNC machine movement. Besides, some auxiliary instructions are inserted into the NC programs including the arc striking or arc extinguishing to complete sequential control of the deposition and rolling process. By doing this, the hybrid manufacturing process is controlled automatically.

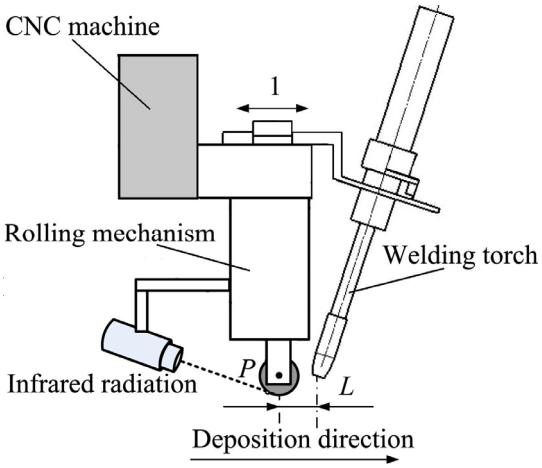

Fig. 4 Schematic of deposition and rolling experimental equipment

The motion of the metamorphic rolling mechanism was tested and the working-phase configurations for different part features described in section 2.1 were shown in Fig.5.

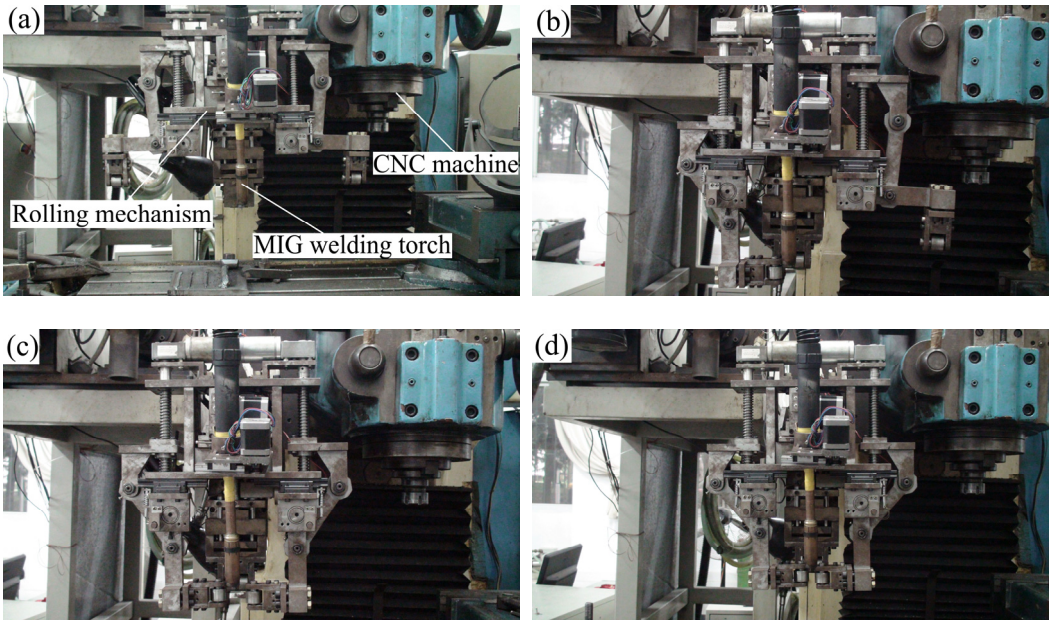

Fig.5 Photos of metamorphic rolling mechanism at different work condition, (a) one roller, (b) two rollers, (c) three rollers for thin wall with thickness of 10 mm, (d) three rollers for thin wall with thickness of 6 mm.

Using 1.2 mm diameter low alloy wire as welding material, single beads were deposited and rolled by moving the welding torch along a straight line. Ar (99.999%) gas was the shielding gas with a flow rate of 18 L/min. The influence of rolling force and rolling temperature on the bead relative deformation was studied. Then, experiments were carried out to control height and width of thin-walled part by the transformation of metamorphic rolling mechanism configurations. The rolled and unrolled muti-layered single bead walls with the length of 120 mm were deposited for comparison. The average rolling temperature was about 940 °C for the thin wall part deposition.

As one layer was deposited, the beads were air-cooled to 200 °C. Then, the welding torch was moved for the next layer deposition. The experiments main parameters were listed in Table 1.

Table 1 Parameters of deposition and rolling

	single bead	thin-wall part
Wire feed (m/min)	4.8	
Welding speed (mm/min)	900	
Welding power (kw)	14.5	
Pulse frequency (Hz)	300	
Pulse width (ms)	0.7	
Shielding gas flow rate (L/min)	18	
Distance *L* (mm)	28/35/42	28
Preset rolling force (N)	0/2400/2600/2800/3000	0/3000

Experimental results and discussion

As shown in Fig.4, the rolling temperature was measured at point *P* by using infrared radiation. Fig. 6 depicts the rolling temperature at the distance *L* of 28 mm, 35 mm and 42 mm. As one layer was deposited, the rolling temperature increased at the beginning of the layer for the heat accumulation. Because the roll continued to move a distance of *L* after the arc extinguishing, the heat lost results in rolling temperature decrease at the ending of the layer. The average rolling temperature was 941 °C, 837 °C and 770 °C at the distance *L* of 28 mm, 35 mm and 42 mm, respectively. Generally, the hot rolling temperature of low carbon steel is 50-100 °C above the A_{r3}, and then the steel was rapidly cooled to phase transition temperature to obtain fine-grained structure and improved mechanical property [14, 15]. Thus, the proper *L* is 28 mm at the deposition condition.

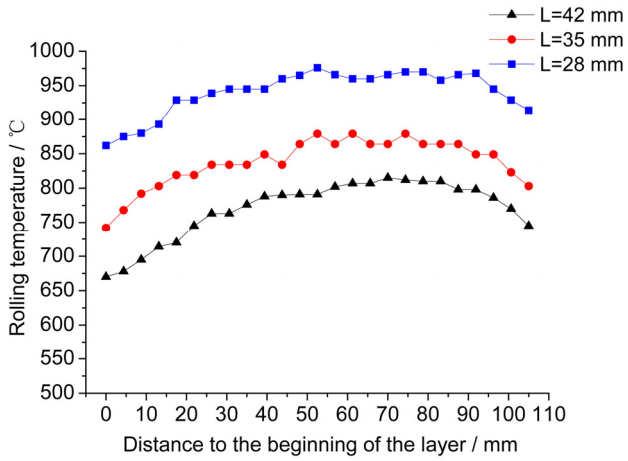

Fig. 6 The rolling temperature curve at different distance L

Fig.7 depicts photographs of the bead at different preset rolling force when the distance L is 28 mm. It can be seen that the bead upper surface becomes more flat at the preset rolling force of 3000 N. As shown in Fig.8, the rolling force and rolling temperature has much effect on the bead relative deformation ε, which is given as Eq. (7).

$$\varepsilon=\frac{h_0-h_1}{h_0} \tag{7}$$

Where h_0 is the average height of the unrolled bead and h_1 is the average height of the rolled bead.

As the increase of the rolling force and rolling temperature, the bead relative deformation increases. When the distance L is 28 mm, the deposition relative deformation are 12.6%, 14.1%, 15.8% and 18.6% at the measured average rolling force of 2425 N, 2631 N, 2830 N and 3014 N, respectively.

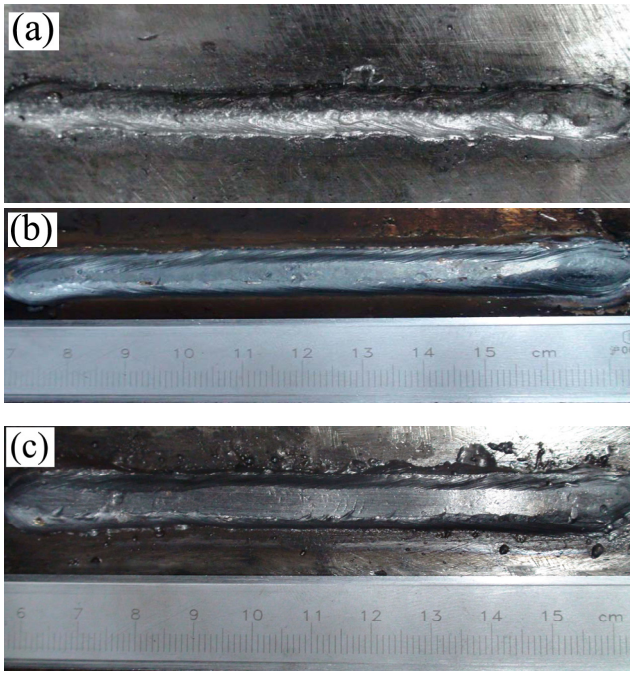

Fig. 7 Photographs of the bead at different preset rolling force, (a) unrolled bead, (b) 2600 N, (c) 3000 N

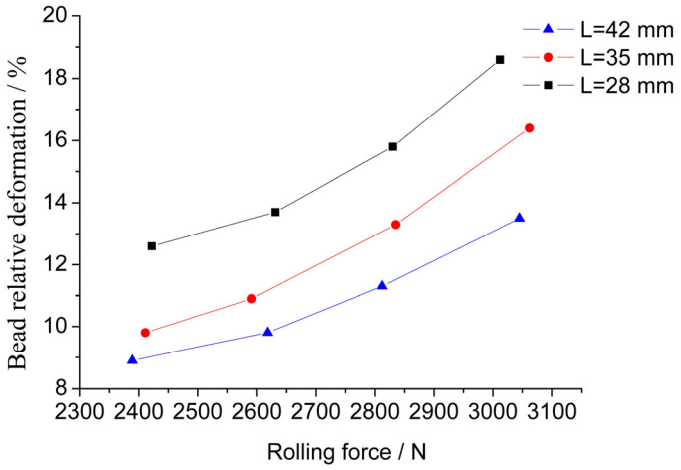

Fig. 8 The bead relative deformation at different rolling force

Photographs of the thin-walled parts with and without horizontal rolling are presented in Fig. 9. The rolled thin-walled part upper surface is flat and smooth while the unrolled one is uneven. Five points for each layer are selected to measure the bead height and the maximum height absolute error. The results are shown in Fig. 10. As the number of deposited layers increases, the uneven surface has a cumulative effect on the accuracy of the component in the Z-direction. For the deposition of subsequent layers, the uneven surface results in the fluctuation of the distance between the welding torch and the deposited layer, which disturbs the arc stability. The average height is 30.8 mm and the maximum height absolute error is about 2.4 mm for the sixteen-layered thin wall without rolling. On the contrary, the average height is 25.1 mm and the maximum height absolute error is about 0.2 mm for the rolled one, and no large height fluctuation appears. Conventionally, each layer was face milled after deposition to remove scallops and stack up of errors. Compared with the machining method, the deposition and rolling processes are carried out simultaneously, which makes time and materials saving possible.

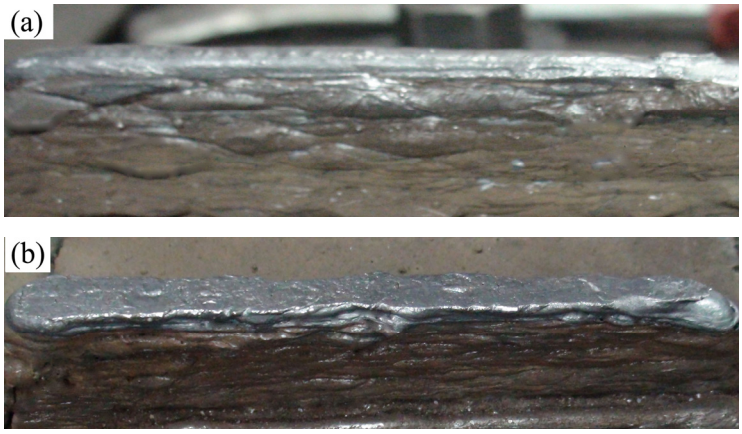

Fig.9 Photographs of the sixteen-layered thin wall with and without horizontal rolling, (a) the thin wall without rolling, (b) the thin wall with rolling

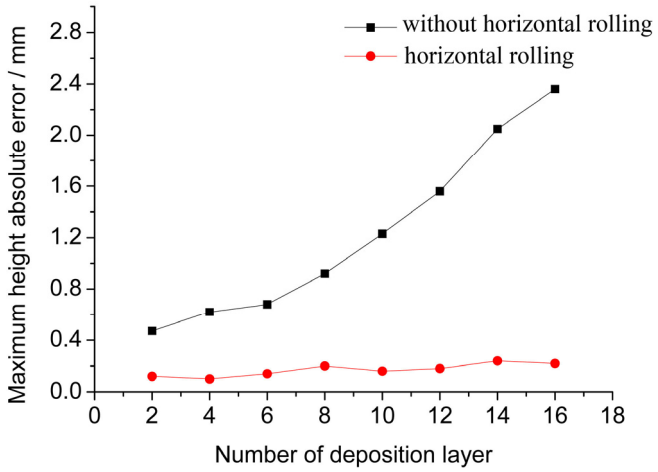

Fig.10 The maximum height absolute error of the thin-walled part

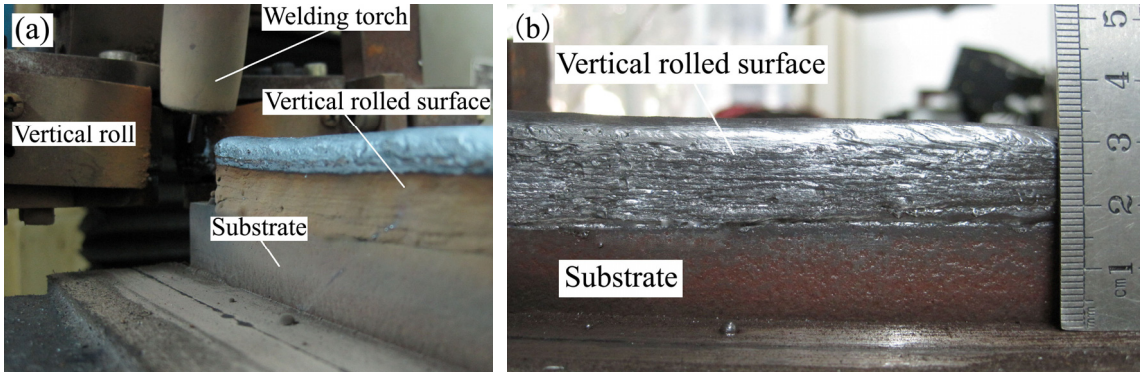

Fig. 11 Photographs of the thin-walled parts with vertical rolling, (a) side view of the thin-walled part with rolling, (b) front view of the thin-walled part with rolling

Table 2 Detailed error analysis for the beads with and without vertical rolling

Deposition layer	Average width(mm)		Maximum width absolute error (mm)		Mean square deviation (mm)	
	a*	b	a	b	a	b
First	8.73	8.67	0.36	0.06	0.14	0.03
Second	8.92	8.71	0.19	0.10	0.08	0.04
Fourth	8.83	8.76	0.33	0.12	0.13	0.02
Sixth	9.07	8.78	0.45	0.07	0.20	0.05
Eighth	9.14	8.70	0.42	0.04	0.18	0.02

* a is the condition for the thin-walled parts without vertical rolling. b is the condition for the thin-walled parts with vertical rolling.

Photographs of thin-walled parts with and without vertical rolling are presented in Fig. 11 and Fig.9a respectively. It can be seen that the lateral surface becomes flat after vertical rolling. Five points for each layer are selected to measure the bead width and a detailed error analysis for the

beads with and without vertical rolling is shown in Table 2. As the number of deposited layers increases, the average width of bead fluctuates between 8.73 and 9.14 mm and the maximum value of maximum width absolute error is 0.45 mm for the unrolled thin-walled part. On the contrary, the average width fluctuates between 8.67 and 8.78 mm and the maximum value of maximum width absolute error is 0.12 mm for the rolled one, which has small width fluctuation and makes materials saving possible.

Conclusions

This paper aimed at controlling the height and width of beads in metal additive manufacturing process. A new metamorphic rolling mechanism prototype for hybrid deposition and rolling was designed and attempted in the paper, which could change its configuration according to the part features.

(1) The experiments show that the surfaces of bead become flat after rolling. The average height and the maximum height absolute error of the sixteen-layered thin-walled parts without horizontal rolling are 30.8 mm and 2.4 mm respectively while the values are 25.1 mm and 0.2 mm for the rolled one.

(2) The average width fluctuates between 8.73 and 9.14 mm, and the maximum value of maximum width absolute error is 0.45 mm for the thin-walled parts without vertical rolling. On the contrary, the average width fluctuates between 8.67 and 8.78 mm, and the maximum value of maximum width absolute error is 0.12 mm for the rolled one.

(3) Compared with existing additive manufacturing which is freedom deposition process, the parts fabricated by hybrid deposition and rolling have flat surfaces and much smaller dimension fluctuation, which has the advantages of time and materials saving for the net shape of the parts by using post machining. In addition, it is worthwhile to mention that the hybrid deposition and rolling method will be beneficial to refine grain, reduce residual stress, avoid the hot crack and improve the mechanical properties of parts.

Acknowledgments

The authors would like to give their gratitude to Yan Yan, Yanzhao Peng and Qi He for their technical support. This work was financially supported by the National Natural Science Foundation of China under Project No. 51175203.

References

[1] Zhang, H.O., Xu, J., Wang, G.L., Fundamental study on plasma deposition manufacturing. Surface and Coatings Technology, 2002, 171(1-3):112-118.

[2] K.P. Karunakaran, S.Suryakumar, VishalPushpa, et al., Low cost integration of additive and subtractive processes for hybrid layered manufacturing. Robotics and Computer-Integrated Manufacturing.

2010 ,26(5):490-499.
[3] Jun Xiong, Guangjun Zhang, Zhilong Qiu, et al., Vision-sensing and bead width control of a single-bead multi-layer part: material and energy savings in GMAW-based rapid manufacturing. Journal of Cleaner Production, 2013, 41: 82-88.
[4] Yu X, Kim IS, Son JS, Park CE, et al., Fuzzy regression method for prediction and control the bead width in the robotic arc-welding process. Journal of Materials Processing Technology, 2005,164-165:1134-1139.
[5] Kim IS, Son JS, Park CE, et al., A study on prediction of bead height in robotic arc welding using a neural network. Journal of Materials Processing Technology ,2002,130-131(20):229-234.
[6] Cao Yong, Zhu Sheng, Liang Xiubing, et al., Overlapping model of beads and curve fitting of bead section for rapid manufacturing by robotic MAG welding process. Robotics and Computer-Integrated Manufacturing, 2011, 27 (3):641-645.
[7] S. Suryakumar, K.P. Karunakaran, Alain Bernard, et al., Weld bead modeling and process optimization in Hybrid Layered Manufacturing . Computer-Aided Design, 2011 (43):331-344.
[8] Yong-Ak Song, Sehyung Park., Experimental investigations into rapid prototyping of composites by novel hybrid deposition process. Journal of Materials Processing Technology, 2006 ,171(1):35-40.
[9] Xiong, X., Zhang, H. and Wang, G., Metal direct prototyping by using hybrid plasma deposition and milling. Journal of Materials Processing Technology, 2009, 209(1): 124-130.
[10] Karunakaran, K.P. , Pushpa, V.,Akula, S.B., et al., Techno-Economic Analysis of Hybrid Layered Manufacturing. International Journal of Intelligent Systems Technologies and Applications, 2008,4(1-2):161-176.
[11] DAI J S, REES J J., Mobility in metamorphic mechanisms of foldable/erectable kinds. Transactions of ASME, Journal of Mechanical Design, 1999, 121(3):375-382.
[12] Duanling Li, Zhonghai Zhang, J. Michael McCarthy, A constraint graph representation of metamorphic linkages. Mechanism and Machine Theory, 2011, 46:228-238.
[13] Zhang Liping, Wang Delun, Dai Jian S., Biological Modeling and Evolution Based Synthesis of Metamorphic Mechanisms. Transactions of ASME, Journal of Mechanical Design, 2008, 130:072303-1-072303-11.
[14] Zhuang LI, Di WU, Wei LÜ, Effects of Rolling and Cooling Conditions on Microstructure and Mechanical Properties of Low Carbon Cold Heading Steel. Journal of Iron and Steel Research, International, 2012, 19 (11):64-70.
[15] Jeong, W.C., Effect of hot-rolling temperature on microstructure and texture of an ultra-low carbon Ti-interstitial-free steel. Materials Letters, 2008,62 (1):91-94.